BioNanoScience (2025) 15:392
https://doi.org/10.1007/s12668-025-02006-1

RESEARCH

Electronic Waste-Derived Silver Nanoparticles for Drug Interactions and Antioxidant Applications

S. Thiyagaraj[1] · Karthik Kumara[2] · A. S. Giresha[3] · V. Aranganathan[3]

Accepted: 19 May 2025 / Published online: 4 June 2025

Abstract

E-waste printed circuit boards from outdated electronic devices, including old model computers and FM radios, were processed to extract valuable materials. A 1 kg sample of electronic waste printed circuit board was subjected to a leaching process, and the extracted materials were characterized using powder X-ray diffraction, UV–visible spectroscopy, and scanning electron microscopy (SEM). Powder X-ray analysis revealed a cubic crystal structure with space group Fm-3 m (CCDC 9012961). UV–visible spectroscopy indicated energy absorption in the visible range (400–410 nm), and SEM identified a rod-like surface morphology. Molecular docking studies demonstrated interactions between silver nanoparticles and anticancer/antibiotic molecules via cytochrome P450 (CYP P450) enzymes, revealing their potential for drug interactions. Antioxidant activities, including 2,2-diphenyl-1-picrylhydrazyl (DPPH), ferric reducing antioxidant power, and anti-lipid peroxidation assays, were performed, indicating strong antioxidant potential. This study introduces a novel, high-temperature route to obtain phase-pure AgNPs from EWPCBs, with promising applications in drug interaction, oxidative stress reduction, and therapeutic development.

Keywords E-waste-derived silver nanoparticles · UV–vis spectroscopy · X-ray diffraction (XRD) · Molecular docking · SEM and EDX · Antioxidant activity · Lipid peroxidation inhibition

1 Introduction

The synthesis of silver nanoparticles from electronic waste (e-waste) has garnered significant attention due to its dual benefits of waste management and resource recovery. Generally, the chemical reduction, green synthesis [1, 2], bioleaching, and biosynthesis are the very famous methods and are the important sources of silver, gold, and other rich material extractions. Recently, the electronic waste, particularly waste printed circuit boards (WPCBs), contains valuable metals, including silver, gold, and platinum. Efficient recovery of these metals not only mitigates environmental hazards but also provides a sustainable source for nanoparticle synthesis. In these sequences, the nitric acid leaching technique has played a vital role [3–5]. Compared with other methods, this method is very promising for yielding and is also very easy to recover the metals from the e-waste. At the same time, the challenges remain the same in terms of scalability, purity, and consistency of the nanoparticle synthesis. Particularly, there are four major areas that are still not fully addressed, such as low recovery efficiency, high costs and time consumption, impurity of recovered silver, and environmental concerns. Despite all advancements, the gap still exists in developing a highly efficient, scalable, and relatively straightforward method for recovering silver from e-waste with minimal impurities and waste generation [6–8]. In this regard, during the leaching process, Cu, Zn, Pb, and Sn may also dissolve in nitric acid and become metal nitrates. The challenge is to separate $AgNO_3$ from other metal nitrates after leaching through nitric acid. Generally, for this process, a chloride source and a copper source have been used to get selective precipitation (AgCl) or cementation (Cu

✉ S. Thiyagaraj
s.thiyagaraj@jainuniversity.ac.in

[1] Department of Physics and Electronics, School of Sciences, Jain (deemed to-be) University, JC Road, Bangalore 560027, India

[2] Department of Physics & BSN Centre for Nano-Materials and Displays, B.M.S College of Engineering, Bull Temple Road, Bangalore 560019, India

[3] Department of Biochemistry, School of Sciences, Jain (deemed to-be) University, JC Road, Bangalore 560027, India

wire), which comes in handy. In which silver is one that precipitates as AgCl easily or is displaced by copper due to its higher reduction potential, but much more processing time is required to get the final product, and finally, it may also contain Ag with complexes. In this research work, we would like to address this issue with an additional mechanism like introducing a combination of nitric acid leaching with hydrothermal, calcinated temperature routing to get pure silver nanoparticle (AgNP) phase. It is a novel strategy to overcome existing challenges in silver recovery and nanoparticle synthesis. On one hand, the nitric acid effectively dissolves silver from electronic waste, offering a high extraction yield due to its strong oxidative and leaching capabilities [2, 9]. This ensures minimal silver loss compared to other techniques. The nitric acid leaching process is well-suited for large-scale operations due to its straightforward procedural steps and ability to handle significant volumes of e-waste. The technique enables the selective recovery of silver by targeting specific components in the e-waste. On the other hand, through the thermal treatment, like hydrothermal, calcination temperature, the post-leaching silver can be precipitated and reduced with minimal contamination, ensuring high-purity nanoparticles. While maintaining high efficiency, nitric acid leaching with the hydrothermal method with high calcinated temperature reduces the time, chemical processing, and cost associated with silver recovery, making it competitive with other methods [3].

The impact of the research work would bridge the gap between efficient resource recovery and high-quality nanoparticle synthesis, ensuring that the synthesized AgNPs are suitable for critical applications such as drug interactions [10–12], antibacterial activity [13–17], and optical devices and can align with environmental sustainability goals by recycling the acid, neutralizing waste, and preventing hazardous by-products [14]. The high-purity silver obtained through nitric acid leaching serves as an excellent precursor for synthesizing uniform AgNPs with desirable structural, optical, and antibacterial properties. This approach highlights a sustainable and scalable method that could serve as a benchmark for future work in e-waste valorization and nanoparticle technology.

2 Experimental

2.1 Hybrid Approach by Integrating Hydrothermal Synthesis with Nitric Acid Leaching

This study employs a hybrid approach that integrates mechanical separation, thermal treatment, solvent dissolution, and hydrothermal synthesis for the effective processing of electronic waste printed circuit boards (EWPCBs). The hydrothermal process plays a crucial role in breaking down the complex structure of PCBs and ensuring efficient recovery of metals, particularly silver. This method provides a sustainable and scalable approach to e-waste valorization.

2.1.1 Selection of E-Waste Materials and Quantity

A total of 1 kg of e-waste materials was collected for the leaching process. This e-waste material used in this study was specifically selected from outdated electronic devices (especially relays and switches), primarily printed circuit boards (PCBs), silver-plated connectors, and contacts obtained from discarded computer models and miniature FM radios. These sources were chosen due to their Ag-based metal-rich composition and also suitable for efficient recovery and recycling through the proposed methodology, and it is displayed in graphical abstract as shown in Fig. 1. Initially, the manual separation has been taken, where non-essential components such as plastic casings, metal connectors, and other undesired materials were carefully removed mechanically, including plugging and scratching. The remaining e-waste material was finely ground to increase the surface area, thereby enhancing the efficiency of subsequent leaching treatments [3–6].

2.1.2 Thermal Treatment: To Remove Non-Metallic Impurities, Plastics, and Other Volatile Components

To eliminate organic matter and volatile non-metallic impurities, the ground e-waste material underwent thermal treatment. This process involved subjecting the sample to a hot air oven at a temperature of 250 °C for a duration of 3 h. The thermal treatment significantly reduced the organic content, including plastics and moisture, leading to an overall weight reduction of approximately 20%. This step has been essential in preparing the material for effective leaching by removing unwanted organic components and improving metal recovery efficiency.

2.1.3 Dissolution in solvent

Followed by thermal treatment, the e-waste materials were subjected to a dissolution process using a specially prepared solvent mixture. A solution composed of 70 mL of water and 30 mL of ethanol in a 70:30 ratio was prepared to aid in partial dissolution and enhance the dispersion of particles. The thermally treated e-waste samples were introduced into this solution and continuously stirred using a magnetic stirrer for 1 h. The stirring process ensured uniform mixing and facilitated the initial leaching of metal ions, further improving particle dispersion in preparation for hydrothermal processing.

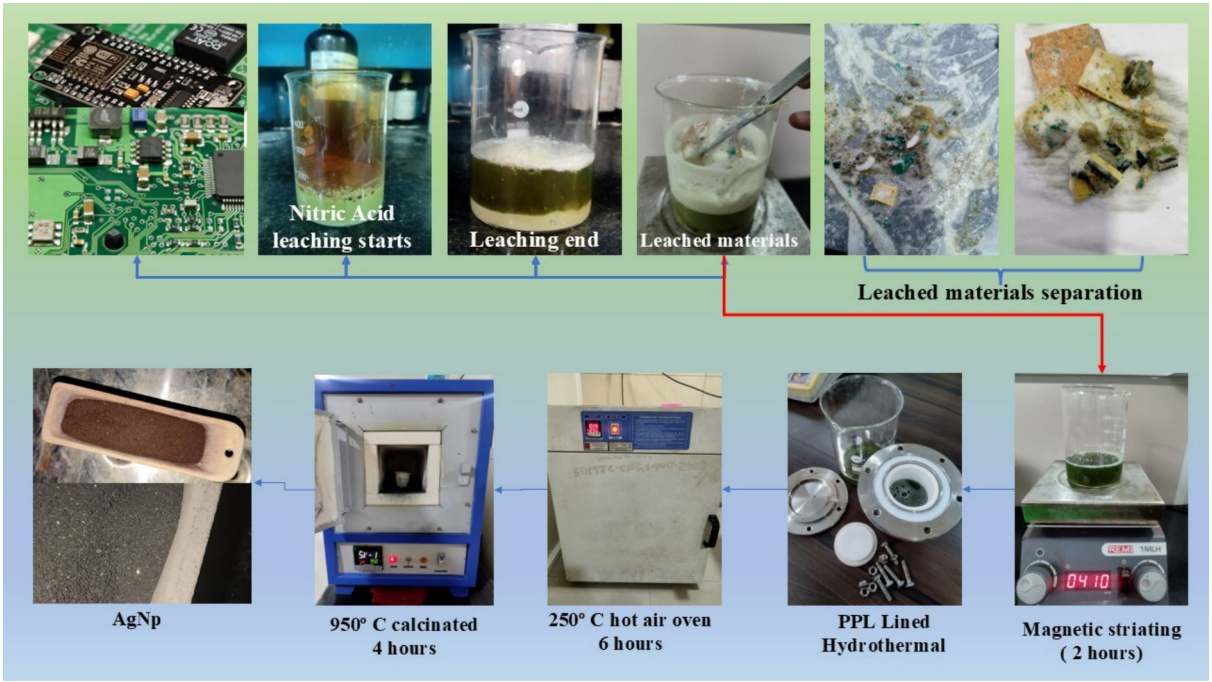

Fig. 1 The leaching procedure of AgNP via nitric acid, hydrothermal and calcinated treatments

2.1.4 Hydrothermal Treatment: Leaching of Silver Nanoparticles and enable the crystallization process

For the final stage, the dissolution-treated sample was transferred into a hydrothermal autoclave to facilitate further metal leaching and crystallization of valuable products. The PPL-Lined Hydrothermal Autoclave Reactor, working pressure: ≤ 3 MPa, heating and cooling rate: ≤ 5 °C/min, and SS Alloy 316, was then placed in a muffle furnace and subjected to a hot air oven at 250 °C for 6 h, and the harvested material was again calcinated at 950 °C for 4 h. The combination of elevated temperature and high pressure within the hydrothermal system enabled the effective breakdown of the material matrix, ensuring enhanced metal recovery, particularly for silver. This process not only optimized leaching efficiency but also promoted the crystallization of desired metal compounds, making it a crucial step in the overall valorization of e-waste materials.

3 Characterization Techniques

The phase and purity identification of AgNPs were analyzed using a powder X-ray diffraction (XRD) technique performed on a Rigaku MiniFlex 600 instrument, employing Cu Kα radiation ($\lambda = 1.5418$ Å) with a scan range of 20–80° and a step size of 0.04°. The optical properties of the silver nanoparticles were studied using a double-beam UV–visible spectrometer (LMSP-UV 1900) with a 520-nm-long light path. Scanning electron microscope (SEM) images of the AgNPs were obtained using a 7100 F SEM instrument. Additionally, with AgNPs, the docking study has been made theoretically through Vina docking to understand the docking performance of the AgNPs with P450 enzyme, and similarly, there are three major experimental in vitro antioxidant activities that we have taken for these present studies, such as free radical scavenging activity, DPPH, ferric reducing antioxidant power (FRAP) assay, and anti-lipid peroxidation activity to confirm its antioxidant nature.

4 Result and Discussion

4.1 Powder X-Ray Diffraction, UV–Visible, and SEM Studies

Space group (Fm-3 m) and cubic structure of the AgNPs are identified using powder X-ray diffraction data via Rietveld refinement method and indicated in Fig. 2a. The "hkl" planes (111), (200), (220), and (311) are identified, and the structure solution has been received through Rietveld refinement, and CCDC 9012961 has been filed in CCDC domain. According to structural refinement, AgNPs have crystallized in cubic nature, and its lattice parameters are $a = b = c = 10.513$ *A*, and $\alpha = \beta = \gamma = 90°$. The $\chi^2 = 1.21$ is the Rietveld global structural conformation indicator, which confirms the good refinement and the single-phase purity. These results are in good agreement with [18–21]. The crystallite size ~ 19

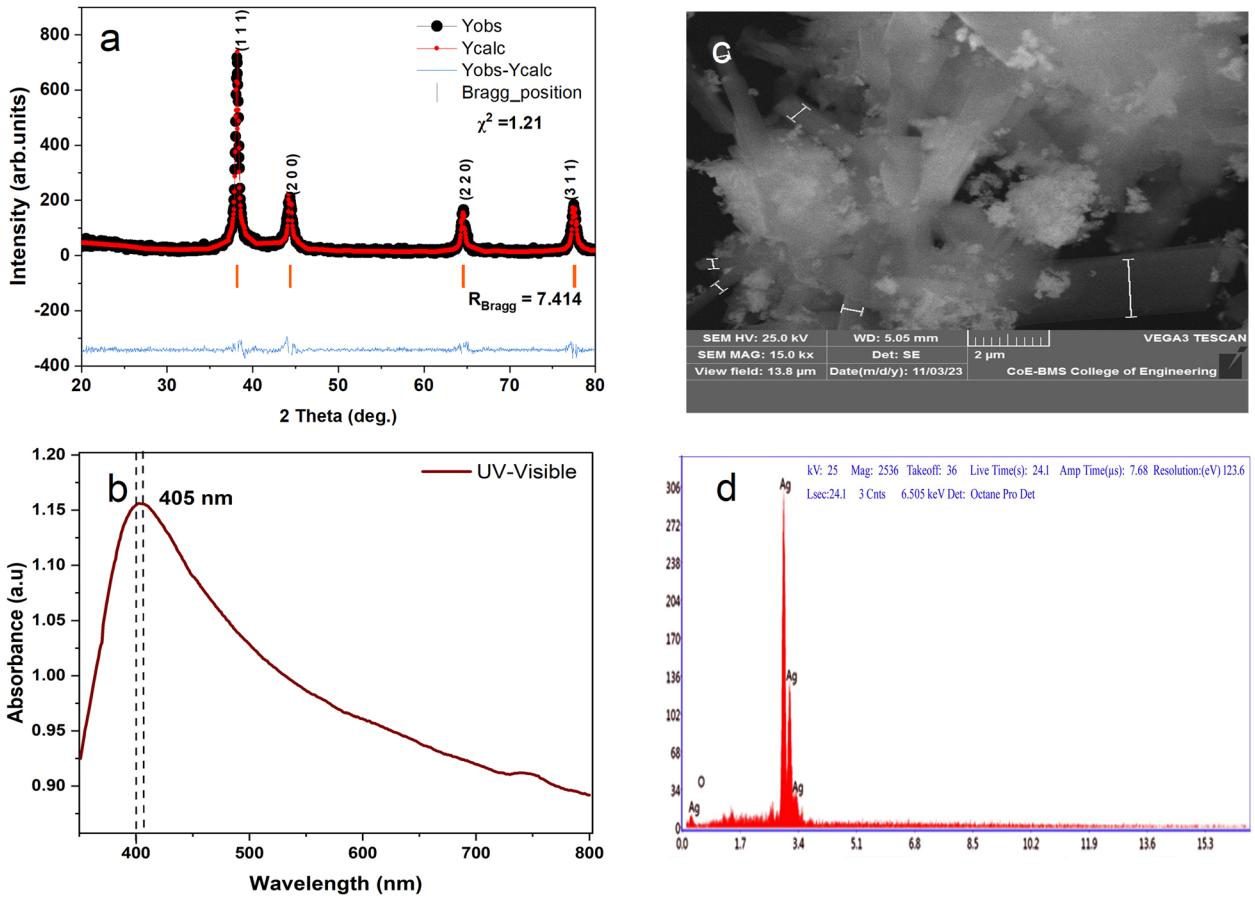

Fig. 2 **a**) Rietveld's structure refinement; **b**) UV–visible absorption spectrum of e-waste AgNP; **c**) *SEM image of* e-waste AgNP; **d**) EDX graph of e-waste AgNP

to 25 nm has been calculated using powder X-ray diffraction data via Scherrer equation $D = K\lambda/\beta cos(2\theta/2)$, where K is the shape factor (typically 0.9), $\lambda = 1.5406\ A$, and β is known as FWHM of peak. These crystallite sizes are also in good agreement with the reported values [22–26]. The UV–Vis absorbance spectrum of AgNPs is displayed in Fig. 2b. The graph indicates that the sharp absorption peaks appear between 400 and 410 nm, which is the visible range. Generally, for the typical Ag crystalline nanoparticle, these absorptions occurred from 400 to 410 nm [27–30]. Particularly, the peak maxima were observed at 405 nm; after that, the broadening extended up to 800 nm. It is due to two reasons: one is based on the shape effect (rods, triangles, or cubes introduce broadening SPR bands) [31], and the other one is based on the calcinated temperature [32]. Using a scanning electron microscope (SEM), Ag particles were examined, and the SEM image is displayed in Fig. 2c. The energy-dispersive X-ray (EDX) spectroscopy was introduced to find the elemental presence, and it is displayed in Fig. 2d, which shows 98% of Ag and 2% of O in weight percentage. Some of low-intensity peaks were observed in the 0.0–1.7 keV range, potentially corresponding to Sn M-lines [33]. However, these were not included in the final elemental quantification due to their low signal-to-noise ratio and ambiguity in distinguishing them from overlapping signals such as oxygen Kα (0.525 keV). Given the high calcination temperature (950 °C) and subsequent purification steps, it is likely that Sn either oxidized and volatilized or remained in trace amounts not contributing to the dominant Ag phase. This is further supported by XRD results, which showed no crystalline phases attributable to Sn-based compounds.

SEM indicates that the Ag particles appear to be aggregated rod-shaped whose breadth ranges from 0.3 to 0.6 µm. In general, this is due to anisotropic (direction-dependent) growth, where the growth rate along one crystallographic axis (like [001]) is faster or slower than others, or if growth along the {100} or {110} faces is faster due to surface modifiers or precursors, the particle elongates along one axis, forming rods. But in this research, we have calcinated at 950 °C, and after leaching, it is the main reason [34], and the residual impurities like Sn, Pb, and other impurities may act as shape-directing agents, altering surface energies and

favoring rod growth [35]. It is also possible that the other evidence is that broadening appears in UV–visible absorption that extends up to 800 nm.

4.2 AgNP Ligand with P450 Enzyme Ligand

This study was designed to investigate the interaction between commonly used therapeutic drugs and metabolic enzymes in the human body. Ciprofloxacin, a widely prescribed antibiotic, and doxorubicin, a potent anticancer agent, were selected due to their clinical importance and different therapeutic roles. Although ciprofloxacin is not extensively metabolized by cytochrome P450 (CYP450) enzymes, it is known to inhibit certain isoforms like CYP1 A2, potentially leading to drug–drug interactions [36]. Doxorubicin, on the other hand, is partially metabolized by enzymes such as CYP3 A4 and CYP2 C8, making it a suitable candidate to evaluate metabolic binding behavior [37]. To explore whether silver nanoparticles (AgNPs) can influence these interactions, we studied the binding affinities of these drugs with key CYP450 isoforms CYP1 A2 (3 WI2), CYP2 C8 (1PQ2), and CYP3 A4 (6MA6) in both the presence and absence of AgNPs [38, 39].

This approach helps us understand whether AgNPs can alter drug metabolism or reduce the risk of harmful enzyme inhibition [25, 40–45]. Generally, the cytochrome P450 enzymes are a large family of enzymes primarily found in the liver, involved in the metabolism of drugs and xenobiotics (foreign compounds). They oxidize drugs, making them easier to eliminate from the body. Using AutoDock Vina, we were able to identify the interaction of the ligand of doxorubicin (an anticancer drug) and ciprofloxacin (an antibiotic drug) with cytochrome P450 and list them in Table 1. Figure 3 shows the interaction of the ligand (AgNPs) with these CYP P450 enzymes, and Fig. 4 shows the ligands (doxorubicin, ciprofloxacin drugs) interaction with CYP P450 enzymes without AgNP and doxorubicin, ciprofloxacin drugs, interaction with CYP P450 (drugs) and AgNPs. This molecular docking study indicates that both ciprofloxacin and doxorubicin interact with key cytochrome P450 enzymes such as CYP1 A2, CYP2 C8, and CYP3 A4. The addition of silver nanoparticles (AgNPs) resulted in slight changes in binding affinity. Notably, AgNPs caused a minor reduction in the binding of ciprofloxacin to CYP1 A2 (from − 7.0 to − 6.9 kcal/mol), potentially lowering the risk of enzyme inhibition. Doxorubicin's binding to CYP2 C8 was marginally reduced (from − 8.3 to − 8.2), while its interaction with CYP3 A4 remained unchanged. These results suggest that AgNPs may subtly modulate drug–enzyme interactions, which could influence drug metabolism and reduce potential drug–drug interaction risks.

Table 1 The AutoDock Vina docking affinity scroe of Doxorubicin and Ciprofloxacin with Cytochrome P450 enzymes

Drugs	Cytochrome P450 enzymes	Affinity (kcal/mol) without AgNPs [25, 40–45]	Affinity (kcal/mol) (with AgNPs)	Syndrome
Doxorubicin	3wi2	− 7.4	− 7.5	CYP1 A2
	1pq2	− 8.3	− 8.2	CYP2 C8
	6 ma6	− 7.5	− 7.5	CYP3 A4
Ciprofloxacin	3wi2	− 7.0	− 6.9	CYP1 A2

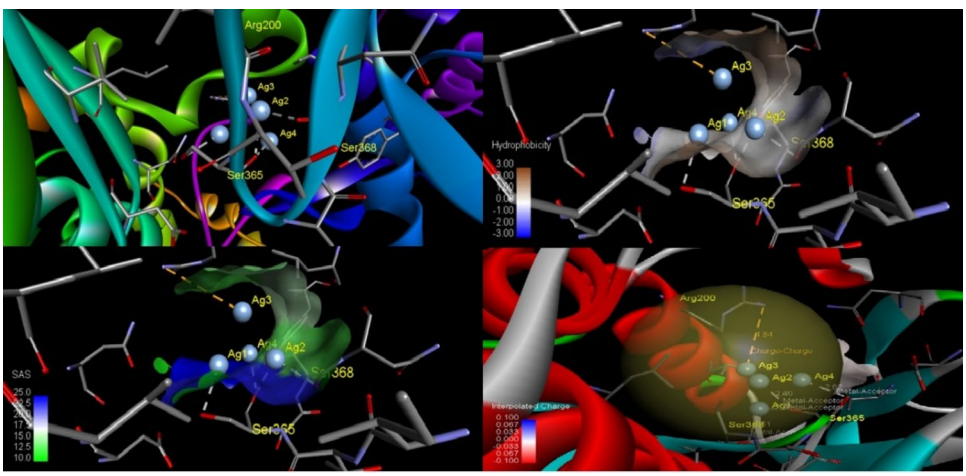

Fig. 3 The AgNP interaction with CYP450 enzyme

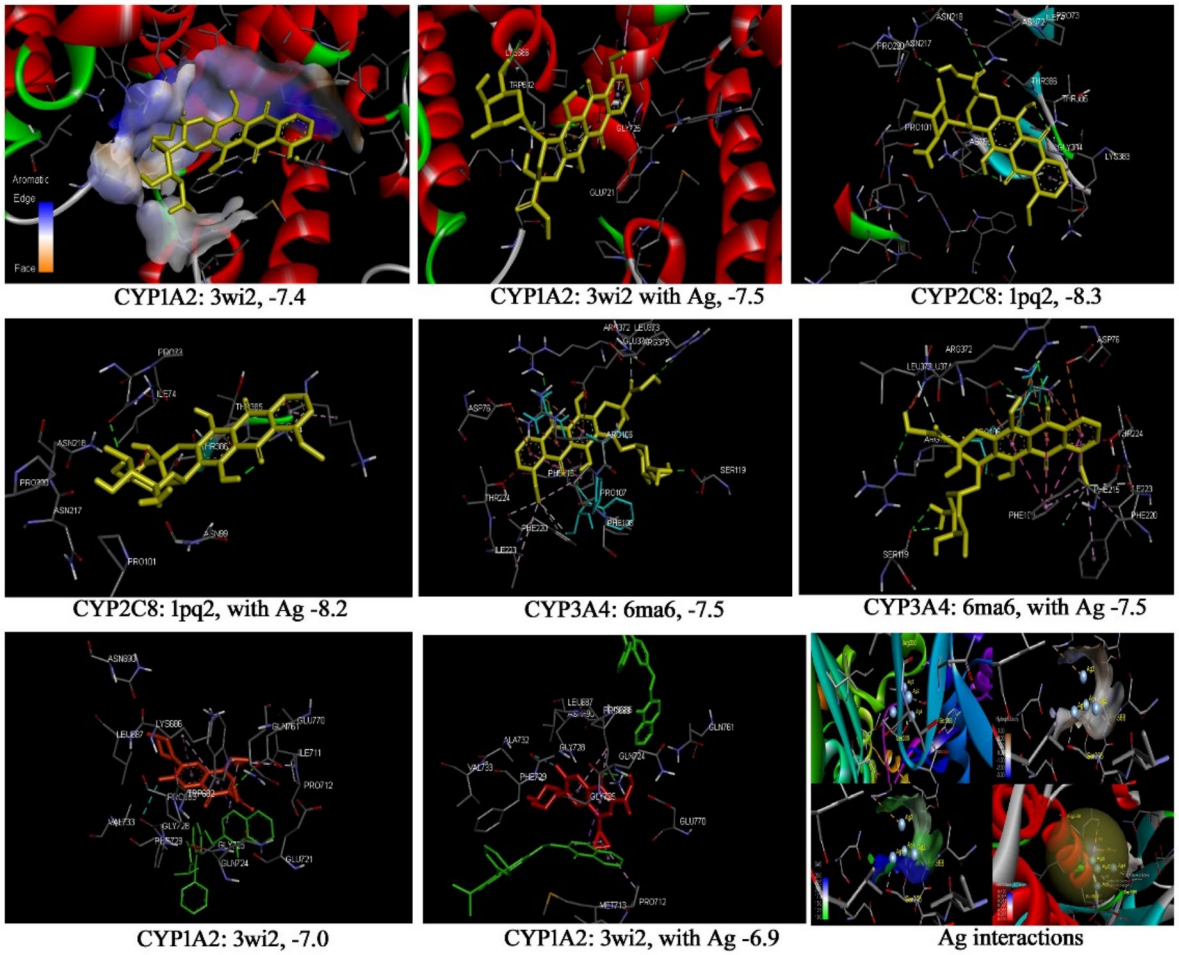

Fig. 4 Interaction of ligand (doxorubicin and ciprofloxacin drugs) with CYP P450 enzymes and doxorubicin, ciprofloxacin drugs, interaction with CYP P450 (drugs) with AgNPs

4.3 Antioxidant Activity and Lipid Peroxidation Inhibition

There are three major antioxidant activities that we have taken for these present studies, such as free radical scavenging activity, DPPH, ferric reducing antioxidant power assay, and anti-lipid peroxidation activity. The activity reports are drawn in Fig. 5.

4.3.1 DPPH (2,2-Diphenyl-1-Picrylhydrazyl) Free Radical Scavenging Activity

The in vitro antioxidant activity of the nanoparticles (AgNPs) was evaluated; for this, the method of Blois [46] with minor modifications has been taken. Various concentrations of AgNPs from 10 to 50 µg were prepared in 100 µL of methanol in a "96-well plate." After that, 200 µL of methanolic DPPH solution of 0.01 mM was added within. The mixture was kept in incubation for 20 min in a dark environment. In this environment, the optical density was 517 nm, with methanol as the blank. Throughout this process, the DPPH was taken as a positive control, and ascorbic acid served as the standard [46–48].

$$\%\ scavenging\ activity = \frac{\text{control O.D} - \text{sample O.D}}{\text{control O.D}} \times 100$$

DPPH scavenging activity is a key indicator of a compound's antioxidant potential, as it measures the ability to neutralize free radicals. Nanoparticles with strong DPPH scavenging activity can effectively donate electrons to stabilize DPPH radicals, thereby reducing oxidative stress in biological systems. This activity is significant because excessive free radicals contribute to aging, inflammation, and the onset of diseases like cancer and neurodegenerative disorders. The nanoparticles synthesized from e-waste, showing high DPPH scavenging capacity, highlight their potential as natural antioxidants for use in therapeutic treatments, cosmetics, and food preservation to combat oxidative damage [49–52].

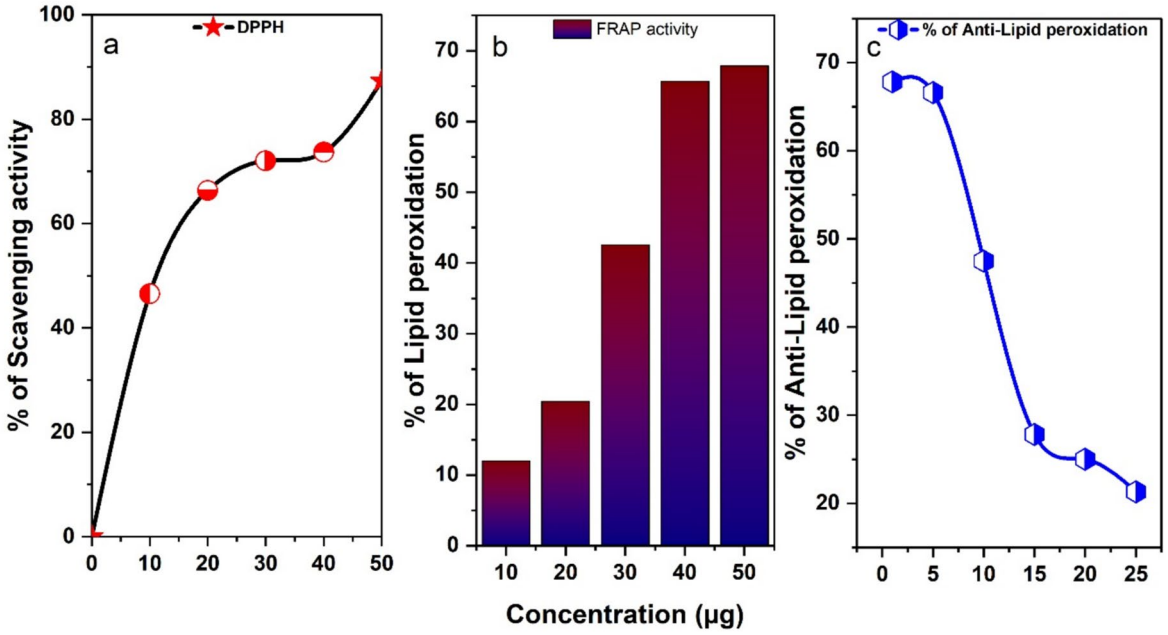

Fig. 5 **a** DPPH scavenging activity of nanoparticles synthesized from e-waste. Different concentrations of NPs were subjected to scavenge 0.01 mM DPPH free radicals. **b**, **c** Reducing power (FRAP) activity of AgNP nanoparticles synthesized. The data represent the mean ± SD, $n = 3$

The antioxidant activity of nanoparticles synthesized from e-waste was evaluated across different concentrations, ranging from 10 to 50 µg, and showed a consistent increase in activity with higher concentrations. The antioxidant activity of the synthesized nanoparticles was concentration-dependent, with activity increasing as the concentration rose from 10 to 50 µg. This nanoparticle exhibited the highest antioxidant activity, suggesting that these nanoparticles confer strong protection against oxidative stress and also demonstrated strong antioxidant activity, starting at 46.56% inhibition at 10 µg and rising to 87.32% at 50 µg, indicating substantial effectiveness at higher concentrations (Fig. 5a). These findings indicate that e-waste-derived nanoparticles can serve as effective antioxidants, showing great promise. These nanoparticles could have valuable applications in industries such as cosmetics, pharmaceuticals, and food preservation, where protection against oxidative stress is essential.

4.3.2 Ferric Reducing Antioxidant Power Assay

Through Oyaizu method [53], the reducing power capacity of the nanoparticles (AgNPs) was assessed with a small modification. Ten to fifty microgram concentrations of AgNPs, 2.5 mL of potassium buffer with 200 mM molarity along with 6.6 pH, and 1% potassium ferricyanide solution (approximately 2.5 mL) were mixed properly for about 1 h, and this mixture was kept incubated at 50 °C for 20 min. Ten percent trichloroacetic acid (2.5 mL) was added, and this solution was centrifuged for 10 min with 3000 rpm. Next, the supernatant solution was mixed with 2.5 mL distilled water and 0.5 mL of $FeCl_3$ solution. The absorbance was recorded at 700 nm against a water blank, and the reducing power was expressed as µM Fe^{2+}, based on the reduction of ferric chloride [28, 48].

FRAP (ferric reducing antioxidant power) activity is a measure of a compound's ability to reduce ferric (Fe^{3+}) ions to ferrous (Fe^{2+}) ions, indicating its antioxidant strength. Nanoparticles exhibiting high FRAP activity demonstrate strong electron-donating capacity, which helps neutralize free radicals and reduce oxidative damage in cells. This is crucial for protecting against diseases related to oxidative stress, such as cancer, cardiovascular disorders, and neurodegeneration. Generally, the high FRAP activity of nanoparticles synthesized from natural extracts underscores their potential as effective antioxidants in pharmaceuticals, skincare products, and food industries, offering natural, safe alternatives to synthetic antioxidants [48]. The same FRAP activity we have checked here for the e-waste AgNPs at concentrations of 10, 20, 30, 40, and 50 µg. The antioxidant capacity of the synthesized nanoparticles followed a concentration-dependent pattern. The results indicate a concentration-dependent trend for antioxidant activity of AgNPs, which exhibited moderate activity across all concentrations, ranging from 12.05 ± 1.4 at 10 µg to 67.86 ± 2.6 at 50 µg (Fig. 5b). These findings suggest that e-waste-derived nanoparticles have promising potential as natural antioxidants,

with potential applications in pharmaceuticals, cosmetics, and food preservation.

4.3.3 Anti-Lipid Peroxidation Activity

The anti-lipid peroxidation activity was evaluated using the thiobarbituric acid reactive substance method [54]. Here, 5 to 25 µg concentrations of AgNPs were pre-incubated in 250 µL of 10% v/v egg homogenate, and the total volume was adjusted to 0.5 mL with distilled water. ALP was initiated by adding 25 µL of 0.07 M $FeSO_4$; this is done after the 30-min incubation at room temperature. Afterward, 750 µL of 20% acetic acid (pH 3.5), 750 µL of 0.8% TBA (in 1.1% SDS), and 25 µL of 20% TCA were added. The mixture was vortexed and heated in a boiling water bath for 60 min, then cooled to room temperature, and 3 mL of 1-butanol was added. The mixture was centrifuged at 3000 rpm for 10 min, and the absorbance of the organic top layer was measured at 532 nm. The anti-lipid peroxidation (ALP) activity was expressed as percentage ALP using the cited formula [47, 55].

$$\text{Percentage ALP} = \frac{1 - \text{sample absorbance}}{\text{control absorbance}} \times 100$$

The anti-lipid peroxidation assay was conducted to evaluate the antioxidant potential of nanoparticles synthesized from e-waste AgNPs; it revealed a significant reduction in lipid peroxidation and was highly effective, with lipid peroxidation levels reducing from 67.8% at 1 µg/mL to 21.3% at 25 µg/mL (Fig. 4c). These results suggest that the synthesized nanoparticles possess the greatest efficacy in reducing lipid peroxidation. This could be due to the AgNPs, or Ag^+ ions are bioactive compounds in nature that are known to neutralize free radicals and prevent oxidative damage. Overall, the data indicates that these nanoparticles could be promising candidates for therapeutic applications aimed at reducing oxidative stress and preventing lipid peroxidation in biological systems. Further research is needed to explore the mechanisms underlying their antioxidant effects and to compare their efficacy with traditional antioxidants.

5 Conclusion

The e-waste printed circuit boards were selectively sourced from outdated computers, circuit boards, miniature radios, and similar electronic devices. For this study, nitric acid leaching process was introduced to extract materials. Leached materials were subsequently characterized using powder X-ray diffraction, UV–visible spectroscopy, and scanning electron microscopy. Additionally, the biological activity of the extracted materials was evaluated, and molecular docking studies were also studied. Powder X-ray diffraction analysis revealed that the leached sample crystallizes in a cubic structure with Fm-3 m space group and the refined structure was deposited in the Cambridge Crystallographic Data Centre (CCDC 9012961). UV–visible spectroscopy confirms the AgNP absorption peaks appear in the visible range (400–410 nm). Through SEM images, a rod-like surface morphology was identified; it may be due to the high calcinated temperature. Furthermore, the molecular docking study was carried out using Vina docking, and it indicates that both ciprofloxacin and doxorubicin interact with key cytochrome P450 enzymes such as CYP1 A2, CYP2 C8, and CYP3 A4. The addition of silver nanoparticles (AgNPs) resulted in slight changes in binding affinity. Notably, AgNPs caused a minor reduction in the binding of ciprofloxacin to CYP1 A2 (from − 7.0 to − 6.9 kcal/mol), potentially lowering the risk of enzyme inhibition. Doxorubicin's binding to CYP2 C8 was marginally reduced (from − 8.3 to − 8.2), while its interaction with CYP3 A4 remained unchanged. These results suggest that AgNPs may subtly modulate drug–enzyme interactions, which could influence drug metabolism and reduce potential drug–drug interaction risks. Through antioxidant activity and lipid peroxidation inhibition studies, these nanoparticles could be promising candidates for therapeutic applications aimed at reducing oxidative stress and preventing lipid peroxidation in biological systems. Further research is needed to explore the mechanisms underlying their antioxidant effects and to compare their efficacy with traditional antioxidants. Therefore, we would like to conclude that this study underscores the significance of recycling e-waste to extract valuable materials with potential biomedical applications. Further research is recommended to elucidate the mechanisms behind their biological activities and to benchmark their efficacy against conventional antioxidants.

Acknowledgements The author Dr. S.Thiyagaraj would like to thank the CRTA, Minor project, JU/MRP/SOS/31/2022, Jain deemed-to-be University, Bangalore, for providing minor research funds to complete this research work. Author Dr.Karthik Kumara would like to thank B.M.S College of Engineering, Bengaluru, for the financial support under FRPS project no. R&D/FRPS/2022-23/PHY/03.

Author Contribution Dr. Thiyagaraj S. conceptualized and designed the study, supervised the research, and contributed to data analysis and manuscript writing. Karthik Kumara was responsible for experimental work, including the extraction and characterization of silver nanoparticles. A S Giresha performed molecular docking studies and antioxidant assays. V. Aranganathan assisted in data interpretation, manuscript drafting, and revisions. All authors reviewed and approved the final manuscript.

Data Availability No datasets were generated or analysed during the current study.

Declarations

Conflict of Interests None.

Research Involving Humans and Animals Statement None.

Informed Consent None.

Funding Statement None.

Competing interests The authors declare no competing interests.

References

1. Islam, M. A., Jacob, M. V., Antunes, E. (2021). A critical review on silver nanoparticles: From synthesis and applications to its mitigation through low-cost adsorption by biochar. *Journal of Environmental Management, 281*. https://doi.org/10.1016/j.jenvman.2020.111918
2. Ghosh, T., Chattopadhyay, A., Mandal, A. C., Pramanik, S., & Kuiri, P. K. (2020). Optical, structural, and antibacterial properties of biosynthesized Ag nanoparticles at room temperature using Azadirachta indica leaf extract. *Chinese Journal of Physics, 68*, 835–848. https://doi.org/10.1016/j.cjph.2020.10.025
3. Pineda-Vásquez, T., Rendón-Castrillón, L., Ramírez-Carmona, M., & Ocampo-López, C. (2023). From e-waste to high-value materials: Sustainable synthesis of metal, metal oxide, and MOF nanoparticles from waste printed circuit boards. *Nanomaterials, 14*, 69. https://doi.org/10.3390/nano14010069
4. Rendón-Castrillón, L., Ramírez-Carmona, M., Ocampo-López, C., & Gómez-Arroyave, L. (2023). Bioleaching techniques for sustainable recovery of metals from solid matrices. *Sustainability, 15*, 10222. https://doi.org/10.3390/su151310222
5. Psomopoulos, C. S., Kungolos, A., & Di Nardo, A. (2023). Advances in industrial waste reduction. *Applied Sciences, 13*, 1403. https://doi.org/10.3390/app13031403
6. Guo, H., Min, Z., Hao, Y., Wang, X., Fan, J., Shi, P., et al. (2021). Sustainable recycling of LiCoO2 cathode scrap on the basis of successive peroxymonosulfate activation and recovery of valuable metals. *Science of The Total Environment, 759*, Article 143478. https://doi.org/10.1016/j.scitotenv.2020.143478
7. Shirin, S., Jamal, A., Emmanouil, C., & Yadav, A. K. (2021). Assessment of characteristics of acid mine drainage treated with fly ash. *Applied Sciences, 11*, 3910. https://doi.org/10.3390/app11093910
8. Najafi, A., Khoeini, M., Khalaj, G., & Sahebgharan, A. (2021). Synthesis of silver nanoparticles from electronic scrap by chemical reduction. *Mater Res Express, 8*, Article 125009. https://doi.org/10.1088/2053-1591/ac406d
9. Mondal, M. S., Paul, A., & Rhaman, M. (2023). Recycling of silver nanoparticles from electronic waste via green synthesis and application of AgNPs-chitosan based nanocomposite on textile material. *Science and Reports, 13*, 13798. https://doi.org/10.1038/s41598-023-40668-7
10. Hegde, M., Naliyadhara, N., Unnikrishnan, J., Alqahtani, M. S., Abbas, M., Girisa, S., et al. (2023). Nanoparticles in the diagnosis and treatment of cancer metastases: Current and future perspectives. *Cancer Letters, 556*, Article 216066. https://doi.org/10.1016/j.canlet.2023.216066
11. Xia, D., Charpentier, N. M., Maurice, A. A., Brambilla, A., Yan, Q., Gabriel, J-C. P. (2022). Sustainable route for Nd recycling from waste electronic components featured with unique element-specific sorting enabling simplified hydrometallurgy. *Chemical Engineering Journal, 441,* 135886. https://doi.org/10.1016/j.cej.2022.135886
12. Manjusha, V., Rajeev, M. R., & Anirudhan, T. S. (2023). Magnetic nanoparticle embedded chitosan-based polymeric network for the hydrophobic drug delivery of paclitaxel. *International Journal of Biological Macromolecules, 235*, Article 123900. https://doi.org/10.1016/j.ijbiomac.2023.123900
13. Rafique, M., Sadaf, I., Tahir, M. B., Rafique, M. S., Nabi, G., Iqbal, T., et al. (2019). Novel and facile synthesis of silver nanoparticles using Albizia procera leaf extract for dye degradation and antibacterial applications. *Materials Science and Engineering C, 99*, 1313–1324. https://doi.org/10.1016/j.msec.2019.02.059
14. Ahmed, S., Ahmad, M., Swami, B. L., & Ikram, S. (2016). A review on plants extract mediated synthesis of silver nanoparticles for antimicrobial applications: A green expertise. *Journal of Advanced Research, 7*, 17–28. https://doi.org/10.1016/j.jare.2015.02.007
15. Mohamed, M., Hani, B., Koca, F., Unal, G., Rahman, N., Basma, A., et al. (2025). Evaluation of antimicrobial, anticancer, and neuroprotective activities of silver nanoparticles (AgNPs) green-synthesized using a red pigment produced by Streptomyces sp. A23 strain isolated from Algerian bee pollen. *Journal of the Serbian Chemical Society,* 8–8. https://doi.org/10.2298/JSC240915008M
16. Koca, F. D., Halici, M. G., Işik, Y., & Ünal, G. (2024). Green synthesis of Ag-ZnO nanocomposites by using *Usnea florida* and *Pseudevernia furfuracea* lichen extracts and evaluation of their neurotoxic effects. *Inorganic and Nano-Metal Chemistry, 54*, 818–825. https://doi.org/10.1080/24701556.2022.2078351
17. Koca, F. D., Demırbas, A., Halıcı, M. G., & Ocsoy, İ. (2024). Bio-synthesis of graphene oxide-decorated silver nanocomposites using Usnea antarctica and Umbilicaria antarctica from Antarctic Peninsula and evaluation of their antimicrobial activities. *Rend Lincei Sci Fis Nat, 35*, 513–522. https://doi.org/10.1007/s12210-024-01246-9
18. Rajahalme, J., Perämäki, S., Budhathoki, R., & Väisänen, A. (2021). Effective recovery process of copper from waste printed circuit boards utilizing recycling of leachate. *JOM Journal of the Minerals Metals and Materials Society, 73*, 980–987. https://doi.org/10.1007/s11837-020-04510-z
19. Rajahalme, J., Perämäki, S., Väisänen, A. (2022). Separation of palladium and silver from e-waste leachate: Effect of nitric acid concentration on adsorption to thiol scavenger. *Chemical Engineering Journal Advances, 10*. https://doi.org/10.1016/j.ceja.2022.100280
20. Guo, Q., Peng, Y., Chao, K. (2022). Raman enhancement effect of different silver nanoparticles on salbutamol. *Heliyon, 8*. https://doi.org/10.1016/j.heliyon.2022.e09576
21. Tailor, G., Yadav, B. L., Chaudhary, J., Joshi, M., Suvalka, C. (2020). Green synthesis of silver nanoparticles using Ocimum canum and their anti-bacterial activity. *Biochemistry and Biophysics Reports, 24*. https://doi.org/10.1016/j.bbrep.2020.100848
22. Rasheed, T., Bilal, M., Iqbal, H. M. N., & Li, C. (2017). Green biosynthesis of silver nanoparticles using leaves extract of Artemisia vulgaris and their potential biomedical applications. *Colloids and Surfaces. B, Biointerfaces, 158*, 408–415. https://doi.org/10.1016/j.colsurfb.2017.07.020
23. Khodashenas, B., & Ghorbani, H. R. (2019). Synthesis of silver nanoparticles with different shapes. *Arabian Journal of Chemistry, 12*, 1823–1838. https://doi.org/10.1016/j.arabjc.2014.12.014
24. Oprica, L., Andries, M., Sacarescu, L., Popescu, L., Pricop, D., Creanga, D., et al. (2020). Citrate-silver nanoparticles and their impact on some environmental beneficial fungi. *Saudi J Biol Sci, 27*, 3365–3375. https://doi.org/10.1016/j.sjbs.2020.09.004
25. Jyoti, K., Baunthiyal, M., Singh, A. (2016). Characterization of silver nanoparticles synthesized using Urtica dioica Linn. leaves

and their synergistic effects with antibiotics. *Journal of Radiation Research and Applied Sciences, 9*, 217–27. https://doi.org/10.1016/j.jrras.2015.10.002
26. Ahmed, S., Saifullah, Ahmad, M., Swami, B. L., Ikram, S. (2016). Green synthesis of silver nanoparticles using Azadirachta indica aqueous leaf extract. *Journal of Radiation Research and Applied Sciences, 9,* 1–7. https://doi.org/10.1016/j.jrras.2015.06.006
27. Alharbi, N. S., Alsubhi, N. S., & Felimban, A. I. (2022). Green synthesis of silver nanoparticles using medicinal plants: Characterization and application. *Journal of Radiation Research and Applied Science, 15*, 109–124. https://doi.org/10.1016/j.jrras.2022.06.012
28. Uddin, I., Ahmad, K., Khan, A. A., & Kazmi, M. A. (2017). Synthesis of silver nanoparticles using Matricaria recutita (Babunah) plant extract and its study as mercury ions sensor. *Sens Biosensing Res, 16*, 62–67. https://doi.org/10.1016/j.sbsr.2017.11.005
29. Fatimah, I. (2016). Green synthesis of silver nanoparticles using extract of Parkia speciosa Hassk pods assisted by microwave irradiation. *Journal of Advanced Research, 7*, 961–969. https://doi.org/10.1016/j.jare.2016.10.002
30. Verma, A., & Mehata, M. S. (2016). Controllable synthesis of silver nanoparticles using Neem leaves and their antimicrobial activity. *Journal of Radiation Research and Applied Science, 9*, 109–115. https://doi.org/10.1016/j.jrras.2015.11.001
31. Yallappa, S., Manjanna, J., Peethambar, S. K., Rajeshwara, A. N., & Satyanarayan, N. D. (2013). Green synthesis of silver nanoparticles using Acacia farnesiana (sweet acacia) seed extract under microwave irradiation and their biological assessment. *Journal of Cluster Science, 24*, 1081–1092. https://doi.org/10.1007/s10876-013-0599-7
32. Gharibshahi, L., Saion, E., Gharibshahi, E., Shaari, A., & Matori, K. (2017). Structural and optical properties of Ag nanoparticles synthesized by thermal treatment method. *Materials, 10*, 402. https://doi.org/10.3390/ma10040402
33. Newbury*, D. E., Ritchie, N. W. M. (2013). Is scanning electron microscopy/energy dispersive <scp>X</scp> -ray spectrometry (<scp>SEM</scp> / <scp>EDS</scp>) quantitative? *Scanning, 35,* 141–68. https://doi.org/10.1002/sca.21041
34. Mahmoud, M. A., El-Sayed, M. A., Gao, J., & Landman, U. (2013). High-frequency mechanical stirring initiates anisotropic growth of seeds requisite for synthesis of asymmetric metallic nanoparticles like silver nanorods. *Nano Letters, 13*, 4739–4745. https://doi.org/10.1021/nl402305n
35. Wiley, B., Sun, Y., Mayers, B., Xia, Y. (2005). Shape-controlled synthesis of metal nanostructures: The case of silver. *Chemistry – A European Journal, 11*, 454–63. https://doi.org/10.1002/chem.200400927
36. Pan, W., Zheng, L., Gao, J., Ye, L., Chen, Z., Liu, S., et al. (2022). SIS3 suppresses osteoclastogenesis and ameliorates bone loss in ovariectomized mice by modulating Nox4-dependent reactive oxygen species. *Biochemical Pharmacology, 195*, Article 114846. https://doi.org/10.1016/j.bcp.2021.114846
37. Ohya, S., Kajikuri, J., Kito, H., Matsui, M. (2023). Down-regulation of CYP3A4 by the KCa1.1 inhibition is responsible for overcoming resistance to doxorubicin in cancer spheroid models. *International Journal of Molecular Sciences, 24*, 15672. https://doi.org/10.3390/ijms242115672
38. Nie, P., Zhao, Y., & Xu, H. (2023). Synthesis, applications, toxicity and toxicity mechanisms of silver nanoparticles: A review. *Ecotoxicology and Environmental Safety, 253*, Article 114636. https://doi.org/10.1016/j.ecoenv.2023.114636
39. Almatroudi, A. (2020). Silver nanoparticles: Synthesis, characterisation and biomedical applications. *Open Life Sci, 15*, 819–839. https://doi.org/10.1515/biol-2020-0094
40. Wasukan, N., Kuno, M., & Maniratanachote, R. (2019). Molecular docking as a promising predictive model for silver nanoparticle-mediated inhibition of cytochrome P450 enzymes. *Journal of Chemical Information and Modeling, 59*, 5126–5134. https://doi.org/10.1021/acs.jcim.9b00572
41. Shahzadi, A., Eyileten, C., Postula, M., Tanoglu, E. G., Karatas, O. F., Basci, A. B., et al. (2023). Investigation of doxorubicin combined with ciprofloxacin-induced cardiotoxicity: From molecular mechanism to fundamental heart function. *Naunyn-Schmiedeberg's Archives of Pharmacology, 396*, 1547–1561. https://doi.org/10.1007/s00210-022-02331-2
42. Paswan, S. K., Kumari, S., Kar, M., Singh, A., Pathak, H., Borah, J. P., et al. (2021). Optimization of structure-property relationships in nickel ferrite nanoparticles annealed at different temperature. *Journal of Physics and Chemistry of Solids,* 151. https://doi.org/10.1016/j.jpcs.2020.109928
43. Nischitha, R., Vasanthkumari, M. M., Kumaraswamy, B. E., Shivanna, M. B. (2020). Antimicrobial and antioxidant activities and chemical profiling of Curvularia tsudae endophytic in Cynodon dactylon (L.) Pers. *3 Biotech,* 10. https://doi.org/10.1007/s13205-020-02250-0
44. Porubsky, P. R., Battaile, K. P., & Scott, E. E. (2010). Human cytochrome p450 2E1 structures with fatty acid analogs reveal a previously unobserved binding mode. *Journal of Biological Chemistry, 285*, 22282–22290. https://doi.org/10.1074/jbc.M110.109017
45. Deng, L.-J., Hu, L.-P., Peng, Q.-L., Yang, X.-L., Bai, L.-L., Yiu, A., et al. (2014). Hellebrigenin induces cell cycle arrest and apoptosis in human hepatocellular carcinoma HepG2 cells through inhibition of Akt. *Chemico-Biological Interactions, 219*, 184–194. https://doi.org/10.1016/j.cbi.2014.06.003
46. Blois, M. S. (1958). Antioxidant determinations by the use of a stable free radical. *Nature, 181*, 1199–200. https://doi.org/10.1038/1811199a0
47. Rahman, Md. M., Islam, Md. B., Biswas, M., Khurshid Alam, A. H. M. (2015) In vitro antioxidant and free radical scavenging activity of different parts of Tabebuia pallida growing in Bangladesh. *BMC Research Notes, 8*, 621. https://doi.org/10.1186/s13104-015-1618-6
48. Benzie, I. F., & Strain, J. J. (1996). The ferric reducing ability of plasma (FRAP) as a measure of "antioxidant power": The FRAP assay. *Analytical Biochemistry, 239*, 70–76. https://doi.org/10.1006/abio.1996.0292
49. Koca, F. D., Muhy, H. M., & Halıcı, M. G. (2025). Antioxidant and pH-dependent cationic and anionic dye degradation activities of optimum synthesized organic@inorganic Cu hybrid nanoflowers. *International Journal of Phytoremediation, 27*, 412–421. https://doi.org/10.1080/15226514.2024.2424308
50. Koca, F. D., Muhy, H. M., & Halici, M. G. (2024). Catalytic and antioxidant activity of Desmarestia menziesii algae extract based organic@inorganic hybrid nanoflowers. *Journal of Inorganic and Organometallic Polymers and Materials, 34*, 1282–1292. https://doi.org/10.1007/s10904-023-02889-1
51. Koca, F. D., Muhy, H. M., & Halici, M. G. (2023). Synthesis of hybrid Cu nanoflowers by using Tornabea scutellifera lichen extract, and evaluation of their dye degredation, and antioxidant activities. *South African Journal of Botany, 160*, 394–401. https://doi.org/10.1016/j.sajb.2023.07.036

52. Güven, O. C., Kar, M., & Koca, F. D. (2022). Synthesis of cherry stalk extract based organic@inorganic hybrid nanoflowers as a novel fenton reagent: Evaluation of their antioxidant, catalytic, and antimicrobial activities. *Journal of Inorganic and Organometallic Polymers and Materials, 32*, 1026–1032. https://doi.org/10.1007/s10904-021-02160-5
53. Oyaizu, M. (1986). Studies on products of browning reaction. Antioxidative activities of products of browning reaction prepared from glucosamine. *The Japanese Journal of Nutrition and Dietetics, 44*, 307–15. https://doi.org/10.5264/eiyogakuzashi.44.307
54. Ohkawa, H., Ohishi, N., & Yagi, K. (1979). Assay for lipid peroxides in animal tissues by thiobarbituric acid reaction. *Analytical Biochemistry, 95*, 351–358. https://doi.org/10.1016/0003-2697(79)90738-3
55. Ayala, A., Muñoz, M. F., & Argüelles, S. (2014). Lipid peroxidation: Production, metabolism, and signaling mechanisms of malondialdehyde and 4-hydroxy-2-nonenal. *Oxidative Medicine and Cellular Longevity, 2014*, Article 360438. https://doi.org/10.1155/2014/360438